CSCanada
Energy Science and Technology
Vol. 2, No. 1, 2011, pp. 57-61
DOI:10.3968/j.est.1923847920110201.589

ISSN 1923-8460[PRINT]
ISSN 1923-8479[ONLINE]
www.cscanada.net
www.cscanada.org

Simulation Model for High Efficiency of Solar Cells

N.D.Kaushika[1,*]; Reeta[2]

[1]Amity University ,Sector 125 Noida, U.P, India
[2]D.J.(PG) College Baraut, Meerut, India
[*]Corresponding author.
Email: ndkaushika@amity.edu

Received 9 June 2011; accepted 13 July 2011

Abstracts

Simulation model of solar cell device is developed to investigate the optimization of conversion efficiency as a function of its geometrical and materials parameters. An arbitrary profile of impurity distribution in the base region is taken into account by using the method of piece wise integration by exponential approximations .The spatially varying built-in field and mobility are explicitly taken into account. Illustrative numerical computations of quantum & collection efficiencies as well as of solar conversion parameters are presented. Simulation conversion efficiency of mono- crystalline silicon solar cell is in conformity with the 24% efficiency reported in Australia for the PERL structure when reasonably effective (about 2-3%) light trapping is taken into account. The model also supports the structure of multi junction thin film solar cells for ultra high efficiency.

Key words: Solar cell; Mono-crystalline; Simulation model; Ultrahigh efficiency

Kaushika, N.D., & Reeta(2011). Simulation Model for High Efficiency of Solar Cells. *Energy Science and Technology, 2*(1), 57-61.Available from: URL: http://www.cscanada.net/index.php/est/article/view/j.est.1923847920110201.589
DOI: http://dx.doi.org/10.3968/j.est.1923847920110201.589

INTRODUCTION

Solar photovoltaic involves the conversion of the sun's radiant energy into electricity using solar cell. The most common material used for solar cells is silicon. Based on the state and quality of the silicon material there are three types of solar cells that have been produced and marketed:

1. Mono-crystalline Cells: These cells use pure mono-crystalline silicon with almost no defects or impurities. In practice these cells are made from wafers of about 450-500 micrometer thickness and are characterized by the impurity grading in their base region. They are expensive to produce. They have a solar conversion efficiency of about 15-17%.

2. Polycrystalline cells: These cells are produced from slightly poorer grades of mono-crystalline silicon or semiconductor grade silicon. The cells have white speckles on the surface due to impurities. They are comparatively less expensive since simpler processes are involved in their production. They have a solar conversion efficiency of about 10-12%.

3. Amorphous silicon cells/thin film cells: These are often referred to as second generation solar cells and are made from amorphous silicon rather than silicon of crystal structure. They absorb light more effectively than crystalline cells and can, therefore, be thinner. Thin film technology has been successfully used on rigid, flexible, curved and foldable substrates. They have lower cost than crystalline cells but have a lower conversion efficiency of 5-7%. However, the reduced cost often overweighs the reduced efficiency, leading to a net increase in ratio of performance to cost.

Past two decades have witnessed remarkable improvement in solar cell efficiencies. Most of the improvements have originated from improved cell structures and processing techniques). The improvements in Mono-crystalline Cells include effective light trapping schemes, reduction of recombination along the top cell surface using thermal oxide passivation and reduction in bulk recombination by an appropriate rear contact. (Blaker and Green, 1986; Blaker etal.1989 ;Green etal.1990) The most efficient and expensive single-junction silicon cells have been reported to have about 24% efficiency (Wang

etal. 1990). In theoretical understanding of the limits of solar cell efficiencies, several authors (e.g. Fahrenbruch and Bube,1983 and the references therein and Gangadhar and Kaushika,1992) have investigated the quantum and collection efficiencies of graded base solar cells to obtain their solar spectral response .These analyses have not considered in detail the variability's of the built in field as well as of mobility values in the graded base region. .In the present analysis a more rigorous simulation model of graded base solar cell is presented to investigate the effect of geometrical and other parameters related to material processing in the fabrication (Runyan, 1985) of solar cells for their high performance.

1. THE SIMULATION MODEL

The practical solar cell consists of a thin diffused p-type base and long homogenously doped n-type collector. The impurity concentration and its distribution in the base region is considered exponential and Gaussian, gives rise to spatially variable built in field and varying mobility values. For calculating the photocurrent the diffused region is divided into a number of sections, say k, and the impurity profile is approximated by a separate exponential such that

$$\beta_i = \frac{1}{w_i} l_n \frac{N_{i+1}}{N_i} \qquad (i = 1,2,.....k) \tag{1}$$

w_i is the width of the ith section and N_i is the actual impurity concentration at the interface of the ith and (i+1)th section. Each section is characterized by average value of mobility μ_{ni} and diffusion coefficient D_{ni} determined by the impurity concentration. All the distributions may be simulated by the variable values of $(\beta)_i$ which may be expressed as follows:

(i) Uniform distribution :$(\beta)_i = 0$

(ii). Exponential distribution : $(\beta)_i$ = Constant

(iii). Gaussian distribution : $(\beta)_i$ = Variable with i (i=1, 2…..k)

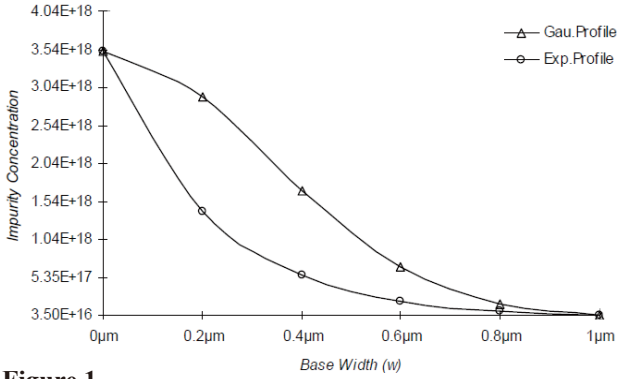

Figure 1
Impurity Profile in a Solar Cell

Built-in-field is given by,

$$E_i = \frac{KT}{q}(\beta)_i \tag{2}$$

The one-dimensional continuity equation for electrons in the ith section of the diffused p-region, with a photon flux F'$_0$ of monochromatic light incident upon the front surface of the cell is given by :

$$D_{ni}\frac{\partial^2 (n)_i}{\partial x^2} + \mu_{ni}E_i\frac{\partial (n)_i}{\partial x} - \frac{(n)_i - (n_{px})_i}{\tau_n} + F_0\alpha\varepsilon exp(-\alpha x) = 0 \quad i = 1,2,....,k. \tag{3}$$

where D_{ni} and μ_{ni} are the diffusion coefficient and mobility values in the ith section, τ_n is life time of electrons, $(n)_i$ is the total concentration of electrons in base, $(n_{px})_i$ is the thermal equilibrium value of electrons in each section of base and α is the absorption coefficient in the semiconductor.

$$\text{and } F_0 = F_0'(1-R) \tag{4}$$

where R is the reflection coefficient.

Equation (3) is 2nd order differential equation, whose solution is

$$(n)_i = A_i\varepsilon exp(m_i x) + B_i\varepsilon exp(\iota_i x) - G_{ni}F_0\varepsilon exp(-\alpha x) + (n_{px})_i \tag{5}$$

Where,

$$m_i = \frac{(\beta)_i}{2} + \sqrt{\frac{(\beta)_i^2}{4} + \frac{1}{D_{ni}\tau_n}} \tag{6}$$

$$l_i = \frac{(\beta)_i}{2} - \sqrt{\frac{(\beta)_i^2}{4} + \frac{1}{D_{ni}\tau_n}} \tag{7}$$

$$\text{and } G_{ni} = D_{ni}^{-1}\left[\alpha + (\beta)_i - \frac{1}{\alpha D_{ni}\tau_n}\right]^{-1} \tag{8}$$

Constants A_i & B_i (i = 1,2…….k) are evaluated using the boundary conditions corresponding to each section. The assumption made to obtain the boundary conditions are:

1. The minority carrier density at the interface of any two sections is continuous:

$$(n)_i\big|_{x=x_i} = (n)_{i+1}\big|_{x=x_i}$$

$$A_i\varepsilon xp(m_i x_i) + B_i\varepsilon xp(l_i x_i) - A_{i+1}\varepsilon xp(m_{i+1}x_i) - B_{i+1}\varepsilon xp(l_{i+1}x_i) - (G_i - G_{i+1})F_0\varepsilon xp(-\alpha x_i) = 0 \tag{9}$$

2. The minority carrier current density at the interface of any two sections is continuous:

$$\left[qD_{ni}\frac{\partial (n)_i}{\partial x} + q\mu_{mi}E_i(n)_i\right]_{x=x_i} = \left[qD_{n(i+1)}\frac{\partial (n)_{i+1}}{\partial x} + q\mu_{n(i+1)}E_{i+1}(n)_{i+1}\right]_{x=xi}$$

$$D_{ni}\left[\frac{\partial (n)_i}{\partial x} - \beta_i(n)_i\right]_{x=xi} = D_{n(i+1)}\left[\frac{\partial (n)_{i+1}}{\partial x} - \beta_{i+1}(n)_{i+1}\right]_{x=xi}$$

$$D_{ni}\begin{bmatrix} A_i m_i\varepsilon xp(m_i x_i) + B_i l_i\varepsilon xp(l_i x_i) + G_i F_0\alpha\varepsilon xp(-\alpha x_i) \\ -A_i\beta_i\varepsilon xp(m_i x_i) - B_i\beta_i\varepsilon xp(l_i x_i) + G_i F_0\beta_i\varepsilon xp(-\alpha x_i) - \beta_i(n_{Px})_i \end{bmatrix}$$

$$= D_{n(i+1)} \begin{bmatrix} A_{i+1} m_{i+1}\, \varepsilon\, xp\,(m_{i+1} x_i) + B_{i+1} l_{i+1}\, \varepsilon\, xp\,(l_{i+1} x_i) + G_{i+1} F_0\, \alpha\, \varepsilon xp\,(-\alpha\, x_{i+1}) \\ -A_{i+1} \beta_{i+1}\, \varepsilon xp\,(m_{i+1} x_{i+1}) \\ -B_{i+1} \beta_{i+1}\, \varepsilon xp\,(l_{i+1} x_i) + G_{i+1} F_0 \beta_{i+1} \varepsilon xp\,(-\alpha x_{i+1}) - \beta_{i+1}\,(n_{Px})_{i+1} \end{bmatrix}$$

$$A_i l_i D_{ni}\, \varepsilon xp(m_i x_i) + B_i m_i D_{ni}\, \varepsilon xp\,(l_i x_i)$$
$$-A_{i+1} l_{i+1} D_{n(i+1)}\, \varepsilon xp\,(m_{i+1} x_i) - B_{i+1} m_{i+1} D_{n(i+1)}\, \varepsilon xp\,(l_{i+1} x_i)$$
$$+G_{i+1} D_{n(i+1)} F_0\,(\alpha + \beta_{i+1})\, \varepsilon xp\,(-\alpha x_i) - G_i D_{ni} F_0\,(\alpha + \beta_i)\, \varepsilon xp\,(-\alpha x_i)$$
$$+\beta_i\,(n_{Pn})_i - \beta_{i+1}\,(n_{Pn})_{i+1} = \quad 0 \tag{10}$$

Equations (9) and (10) give (2k-2) boundary conditions and two more obtained by considering the condition at the surface (x=0) and at the junction (x = w).

$$\sigma\,.(n)_1\big|_{x=0} = D_{n1} \frac{\partial (n)_1}{\partial x}\bigg|_{x=0} + \mu_{n1}\,(E)_1\,(n)_1\big|_{x=0} \tag{11}$$

where σ is the recombination velocity at the $p - n$ surface and is the depth of the junction.

$$(n)_k\big|_{x=w} = 0 \tag{12}$$

Since minority carriers are swept out from the junction by the electric field as soon as possible.

The constants A_t & B_t can be calculated using 2k equations (9-12) , by using the determinant method of solving simultaneous equations.

The electron component of the photo current density is given by,

$$j_{n\,photo} = qD_{nk} \frac{\partial (n)k}{\partial x}\bigg|_{x=w} + q\mu_{nk}\,(E)_k\,(n)_k\big|_{x=w} \tag{13}$$

Quantum efficiency, η_Q and the collection efficiency η_c are

$$\eta_Q = \frac{j_{n\,photo}}{qF_0} \tag{14}$$

$$\eta_c = \frac{j_{n\,photo}}{qF_0\,\{1 - \varepsilon\, xp\,(-\alpha w)\}} \tag{15}$$

The short circuit current j_{pphoto} from the long uniformly doped n-region is given by,

$$j_{pphoto} = \frac{qF_0\, \varepsilon\, xp\,(-\alpha\, w)}{1 + (\alpha\, L_p)^{-1}} \tag{16}$$

where Lp is the diffusion length of holes in then region. The total light generated current is given by,

$$j_L = j_{nphoto} + j_{pphoto} \tag{17}$$

The general expression for total current of photo diode may be written as

$$j = j_0 \left\{ \varepsilon xp \frac{qV}{AKT} - 1 \right\} - j_L \tag{18}$$

At $V = V_{oc}$, j = 0:, the open circuit voltage V_{oc} is therefore, given by

$$V_{oc} = \frac{AKT}{q} \ln \left\{ \frac{j_L}{j_0} + 1 \right\} \tag{19}$$

The power delivered by the junction is given by

$$P = V \times j = V \left\{ j_o \left(\varepsilon xp \frac{qV}{AKT} \right) - j_L \right\} \tag{20}$$

Since $\frac{qV}{AKT} \rangle\rangle 1$

The voltage at the maximum power point is given by ,

$$\left(\frac{dP}{dV}\right)_{V=V_m} = j_o \left(\varepsilon xp \frac{qV_m}{AKT} \right) - j_L + \frac{\frac{j_L}{qV_m}}{AKT}\, j_o\, \varepsilon xp \left(\frac{qV_m}{AKT} \right) = 0$$

$$\left(\frac{qV_m}{AKT} + 1 \right) \varepsilon xp \left(\frac{qV_m}{AKT} \right) = \frac{j_L}{j_o}$$

$$(\mathrm{r} + 1)\varepsilon xp(r) = \frac{j_L}{j_o} \tag{21}$$

where $V_m = \frac{AKT}{q} r$ (22)

and r is the root of the eqn. (21).

$$j_m = j_0 \left\{ \varepsilon xp \left(\frac{qVm}{AKT} \right) \right\} - j_L = j_0\, \varepsilon xp(r) - j_L = -\, j_L \frac{r}{r+1} \tag{23}$$

The load at maximum power point is given by,

$$R_m = \frac{V_m}{j_m}$$

The conversion efficiency is defined by ,

$$\eta = \frac{V_m j_m}{P_{in}} = \frac{P_m}{P_{in}} \tag{24}$$

Where P_m and P_{in} are the maximum power output of the solar cell and the solar irradiance.

2. COMPUTATIONAL RESULTS

The efficiency values of a silicon solar cell having uniform , exponential and Gaussian distribution in the base region are computed corresponding to the solar radiation wavelength range of 0.2-2.0 μm.

Data used are N(0)=3.5x10^{18}cm^{-3}, N(w)=3.5x10^{16}cm^3, w=1μm, τ_n=10^{-7}sec, R=10%, dark current j_0=2.4x10^{-11}A/m^2, P_{in}=1345 W/m^2, AKT/q = 25.84x10^{-3} V and k=5. The results of the calculations for the case of uniform, exponential and Gaussian function impurity profile are shown in table 1,2 & 3 using solar irradiance AM0 in the wavelength range 0.2 to 2.0 μm.

Table 1
Solar Energy Conversion for Uniform Distribution

Parameters	σ= 0.1m / s
j_L(A/m^2)	166.812
j_L/j_0 x 10^{13}(A/m^2)	0.695
V_{oc} (V)	0.764
V_m (V)	0.619
J_m (A/m^2)	160.697
η	8.113

Table 2
Solar Energy Conversion for Different Surface Recombination: Exponential Profile

	σ (m/s)			
Parameters	0.1	10^3	10^4	10^6
$j_L(A/m^2)$	380.564	374.859	362.379	356.615
$j_L/j_0x10^{f3}(A/m^2)$	1.585	1.561	1.509	1.485
V_{oc} (V)	0.785	0.785	0.784	0.783
V_m (V)	0.699	0.699	0.698	0.697
J_m (A/m^2)	367.001	361.493	349.443	343.879
η	19.079	18.783	17.871	17.738

Table 3
Solar Energy Conversion for Different Surface Recombination: Gaussian Profile

	σ (m/s)			
Parameters	0.1	10^3	10^4	10^6
$j_L(A/m^2)$	403.928	389.001	370.114	364.647
$j_L/j_0x10^{f3}(A/m^2)$	1.683	1.62	1.542	1.519
V_{oc} (V)	0.787	0.786	0.785	0.784
V_m (V)	0.701	0.7	0.699	0.698
J_m (A/m^2)	389.338	375.153	356.915	351.629
η	20.305	19.525	18.541	18.146

Table 4
Solar Energy Conversion for Different Base Width: Exponential & Gaussian Profile

	η (%)							
w(μm)	Exponentialσ (m/s)				Gaussianσ (m/s)			
	0.1	10^3	10^4	10^6	0.1	10^3	10^4	10^6
80	23.602	7.341	6.861	6.132	18.405	7.464	6.761	5.932
10	21.727	17.882	16.809	16.656	21.725	16.571	15.758	15.641
1	19.079	18.783	18.136	17.838	20.305	19.525	18.541	18.246
0.1	18.401	18.357	18.160	17.895	18.354	18.354	18.149	17.886
0.001	18.278	18.278	18.278	18.256	18.264	18.264	18.264	18.256

The results of the calculations for the case of a Gaussian and Exponential function impurity profile in the diffused region are shown in table 1,2,3 & 4. It is seen that

(i) The conversion efficiency decreases with increasing surface recombination velocity;

(ii) Conversion Efficiency for uniform distribution is very low as shown in table 1 and efficiencies for exponential and Gaussian profile are slightly different as shown in table 2 and table 3. Hence, the realistic distribution must only be considered and should not always be approximated by a single exponential distribution. These values are quite in agreement with those reported for PERL structure in Australia (Wang etal.1990) if reasonably effective(2-3 %)light trapping is taken into account

(iii) It is seen that towards the lower base width, the effect of surface recombination continuously decreases and at 1nm base width there is approximately no effect of surface recombination as shown in Fig.2 for Gaussian distribution. This view suggests the structure of multi junctions thin film solar cells .

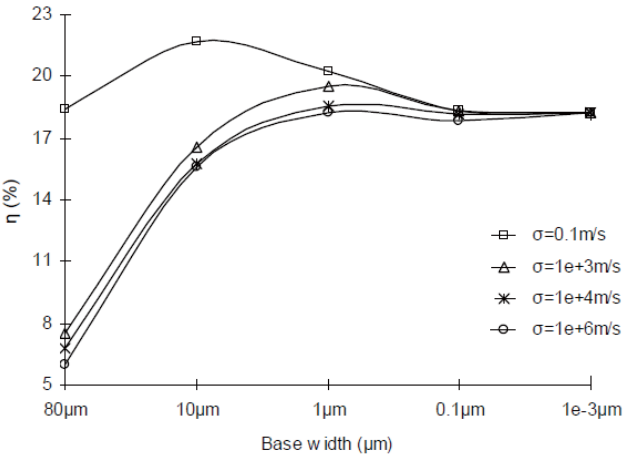

Figure 2
Variation of Conversion Efficiency at Different Surface Recombination for Gaussian Profile

4. ULTRA HIGH EFFICIENCY STRATEGIES & DISCUSSIONS

A major factor limiting the conversion efficiency is single-band-gap. The excess energy is lost as heat through electron phonon scattering and subsequent phonon emission as the hot photo generated carrier relax to their respective band edges; the low energy photons will not create electron-hole pairs.

A more efficient system is that if the low energy photons in sunlight are directed towards the narrow band-gap semi conductors in which they can be utilized. The high energy photons are directed towards the wide band-gap semiconductors where their excess energy dissipation is reduced. The main approach to reduce the losses in solar spectrum, efficiency, therefore, has been to use a stack of cascaded multiple p-n junctions with band gaps better matched to the solar spectrum.

I what follows we calculate the solar cell efficiency for single, two, three, four and five junctions for input solar radiation ranges between 0.3-2.0 μm for AM1.5 solar spectrum and see that efficiency increases by increasing

no. of junctions.

Number of cells	System efficiency (%)	Band gaps(eV)				
1	32.6	1.12				
2	38.5	2.6	1.12			
3	49.7	2.6	1.65	0.72		
4	52.2	2.6	1.65	1.12	0.72	
5	55.0	2.6	2.26	1.65	1.12	0.72

2.6(CdTe); 2.26(GaP); 1.65(a-Si); 1.12(c-Si); 0.72(Ge).
Total solar irradiance=831.8 W/m^2.

Furthermore ,in recent years (eg.Nozik,2001and Shaller and Klimov,2004), it has been proposed and experimentally verified that in some cases the relaxation dynamics of photon-generated carriers may be affected by quantization effects in some semi-conductors like semi-conductor quantum wells, quantum wires, quantum dots, super lattices and nano structures. In these semiconductors the carriers are confined by potential barriers to regions of space that are smaller than or comparable to their de Broglie wave lengths or to the Bohr's radius of excitons in the semi conductor bulk .consequently the hot carriers cooling rates may be dramatically reduced and the rate of impact ionization could become competitive with the cooling rate of carriers .For example, In the quantum dot (QD) case, hot electron cooling is theoretically possible even at arbitrarily low light intensity; this effect is simply called a "photon- bottleneck". It can even be achieved without the qualification of requiring hot phonons (i.e. a non-equilibrium distribution of phonons). Further more it is also anticipated that the slowed cooling could make the rate of exciton multiplication (inverse Auger effect) an important process in QDs. A new possible mechanism for multi-exciton-generation (MEG) was introduced that invokes a coherent superposition of multiple excitonic states meaning that multiple excitons are essentially created instantly upon absorption of high energy photons. Most recently, MEG has been reported in CdSe QDs and PbTe QDs and seven excitons per photon were reported in PbSe QDs at seven times the band gap.

The solar cells based on quantum dots theoretically could convert more than 65% of Sun's energy into electricity, approximately doubling of the efficiency of solar cells. Quantum dots are offering the possibilities for improving the efficiency of solar cells in at least two respects, by extending the band gap of solar cells for harvesting more of the light in the solar spectrum and by generating more charge from a single photon.

REFERENCES

[1] Blakers, A.W., & Green, M. A. (1986). 20-Percent Efficient Silicon Solar Cell. *Appl. Phys. Lett., 48*, 215-217.

[2] Blakers, A.W., Wang, A., Milne, A.M., Jhao, J. & Green, M.A. (1989). 22.8-Percent Efficient Silicon Solar Cell. *Appl. Phys. Lett., 55* (13), 1363-1365.

[3] Fahernbruch, A.L., & Bube, R.H. (1983). *Application of the Transport Equation, In. Fundamentals of Solar Cells*. New York: Academics Press.

[4] Gangadhar, R.B. & Kaushika, N.D. (1992). *Energy convers. Mgmt, 33*(4), 275-278.

[5] Green, M.A., Blaker, A.W., Zhao, J., Milne, A.M., Wang, A., & Dai, X. (1990). Characterization of 23% Efficient Silicon Solar Cells. *IEEE Trans ED, 37*(2), 331-335.

[6] Nozik, A.J. (2001). Spectroscopy and Tot Electron Relaxation Dynamics in Semiconductor Quantum Wells and Quantum Dots. *Annual Review of Physics and chemistry, 52*, 193.

[7] Runyan, W.R. (1965). *Silicon Semiconductor Technology*. New York: McGraw Hill.

[8] Shaller, R.D., & Klimov, V.L. (2004). High Efficiency Carrier Multiplication in Solar Energy Conversion. *Physics Review Letters, 92.*

[9] Wang, A., Zhao, J., & Green, M.A. (1990). 24-Percent Efficient Silicon Solar Cells. *Appl. Phys. Let., 57*, 602-604.